Benemérita Universidad Autónoma de Puebla

and

Dual C-P Institute of High Energy Physics, México

"Higgs physics at futures electron-proton colliders"

Jaime Hernandez -Sanchez

Electrons for the LHC - LHeC/FCCeh and Perle Workshop
October 26-28, 2022, IJCLab-Orsay, France

Outline

- Higgs physics BSM at LHeC and FCC-he.
- 2HDM-III as BSM: model with a four-zero Yukawa texture that controls the FCNC.
- Some interesting channels decays at tree level: H,h,A → bs,τμ, H+ —> cb, ts, decays are sensitive to the pattern of Yukawa texture.
- We show the production e p→q(h,H)ν_e with flavor violating decays of the Higgs bosons (h,H): cross sections, some distributions and cuts.
- We also present the production e- p —> q nu H-, considering H- —> c b

electrons for eh : ERL-e + FCC-hh [LHC]

- **Two 802 MHz Electron LINACs + 2x3 return arcs: using energy recovery in same structure: *sustainable* technology with power consumption < 100 MW** *instead of 1 GW for a conventional LINAC.*
- **Beam dump: no radioactive waste!**
- **high electron polarisation of 80-90%**

Concurrent eh and hh operation with same running time!

Genuine *Twin Collider* idea holds for LHC and FCC-hh.

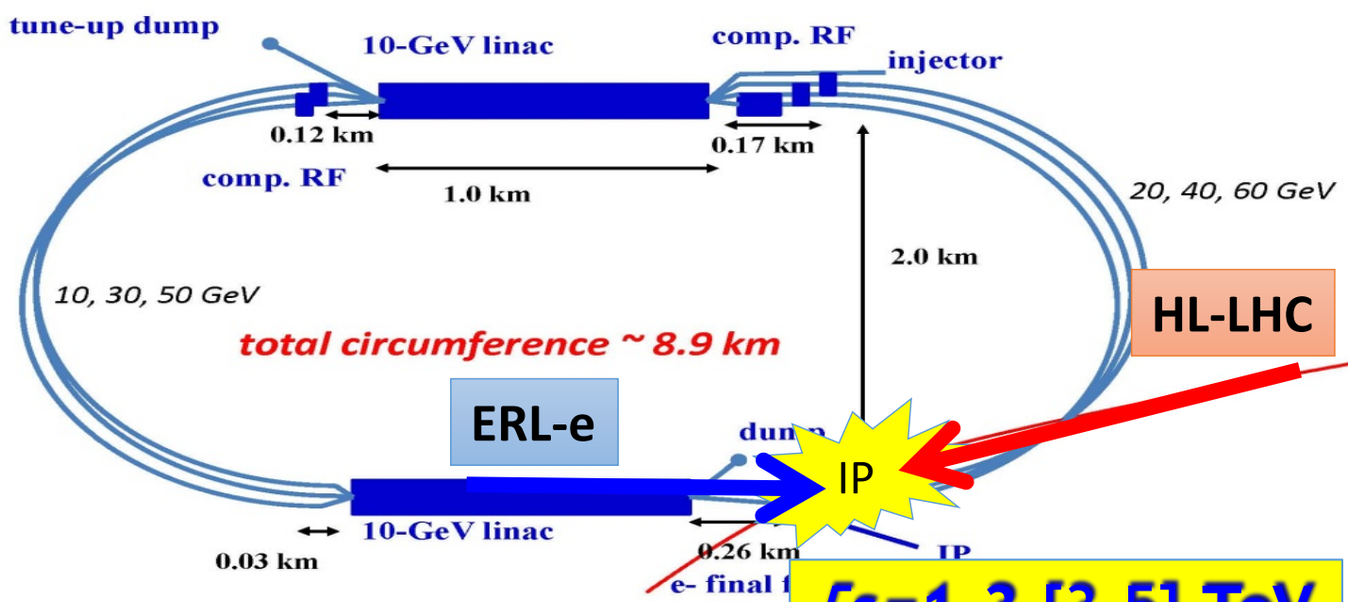

- **ep peak lumi 10^{34} cm s^{-2} s^{-1}** (based on existing HL-LHC design)
- **Operation scenario: F. Bodry et al.** CERN-ACC-2018-0037 [arXiv:1810.13022]
- **LHeC** [FCC-eh] **L= 1000** [2000] **fb^{-1} total collected in 10** [20] **years**
- **'No' pile-up**: <0.1@LHeC; ~1@FCCeh

$\sqrt{s}$=1.3 [3.5] TeV
E_e = 60 GeV
E_p = 7 [50] TeV

ERL design detailed in LHeC CDR: J. Phys. G: Nucl. Part. Phys. 39 (2012) 075001 [arXiv:1206.2913] and CDR update CERN-ACC-Note-2020-0002 [arXiv:2007.14491] and submitted to J. Phys. G → **see Talk #729 by B Holzer & Talk #730 about ERL Facility at Orsay**

Uta Klein, 29.07.22 (Talk at ICHEP 2020, Prague)

Signal

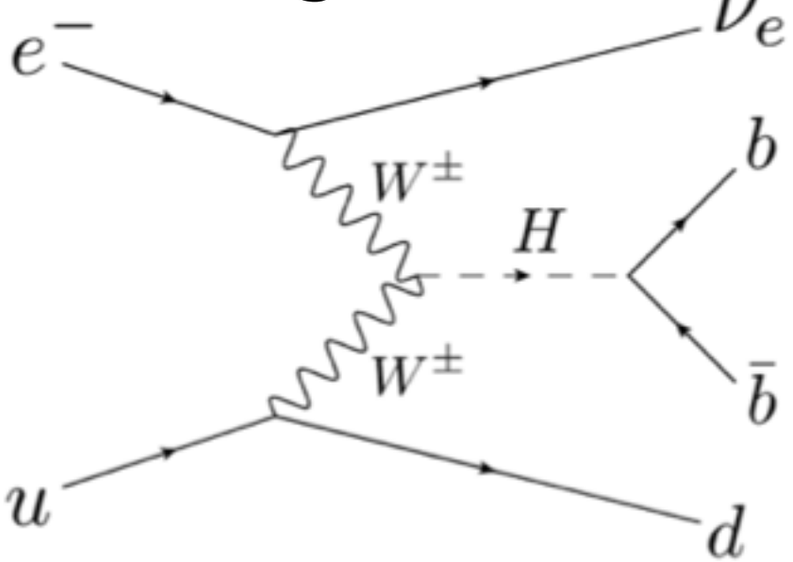

Charged current (CC) H->bb (0.063 pb)

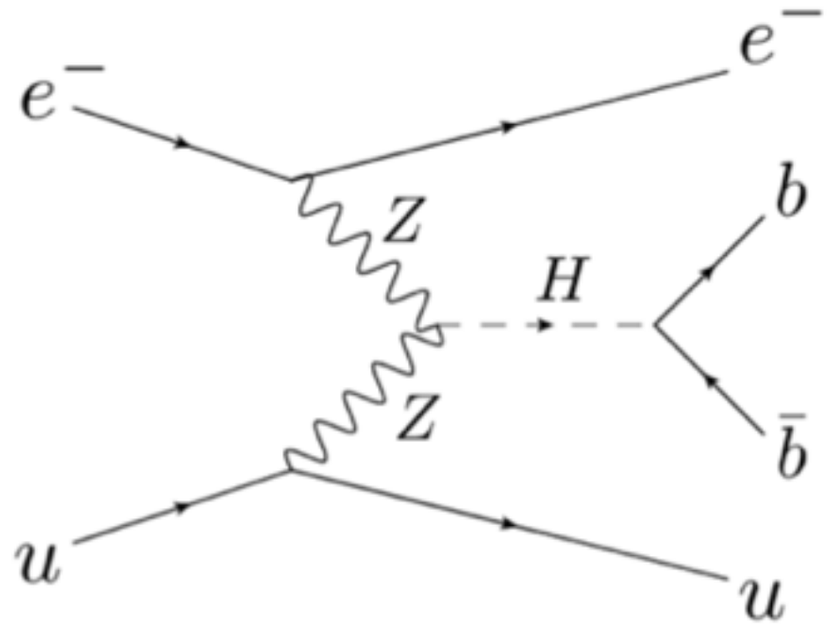

Neutral current (NC) H->bb (0.012 pb)

- CC: H->bb process is chosen as the signal because the cross section is larger than NC: H->bb process and NC rejection cut decreases large number of NC BG.

Background

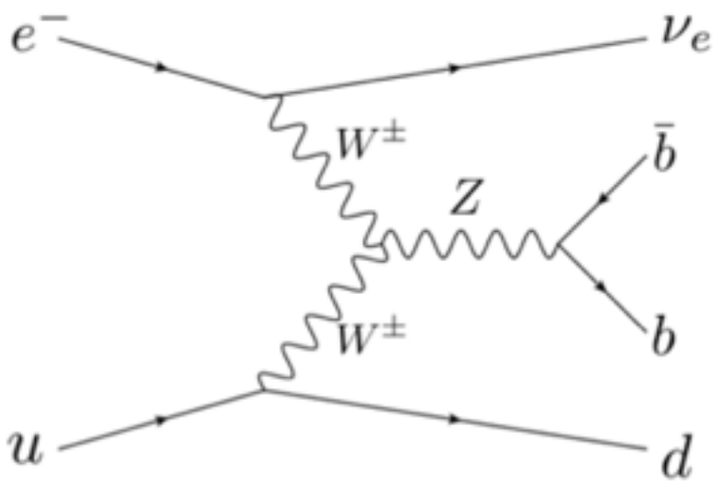

CC Z production (0.29 pb)

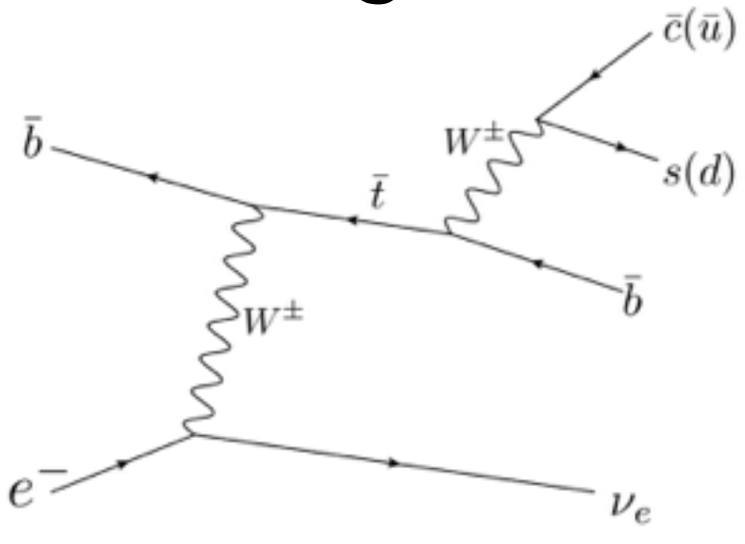

Single top production (0.43 pb)

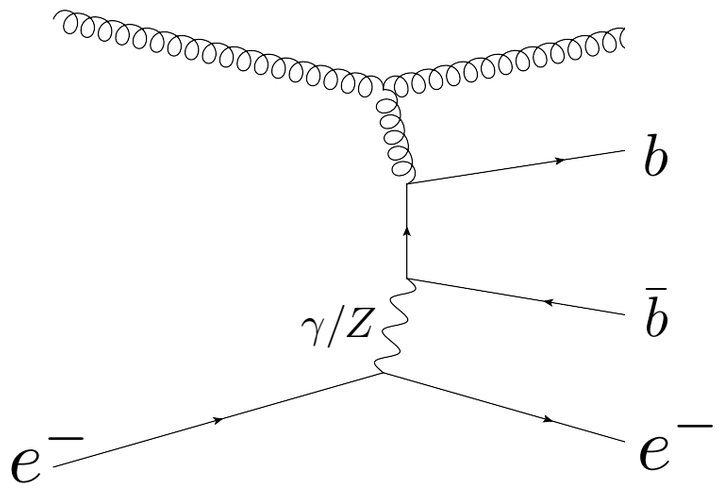

NC multi jets

Analysis Framework and *Detector**

Event generation

- **SM or BSM production**
- **CC & NC DIS background**

by MadGraph5/MadEvent

- **Fragmentation**
- **Hadronization**

by PYTHIA (modified for ep)*

Fast detector simulation

by Delphes

→ test of LHeC detector

S/B analysis → cuts or BDT

- Calculate cross section with tree-level Feynman diagrams (any UFO) using pT of scattered quark as scale (CDR $\hat{s}$) for ep processes with **MadGraph5** ; parton-level x-check CompHep
- Fragmentation & hadronisation uses **ep-customised** Pythia.

- **Delphes 'detector'**

→displaced vertices and signed impact parameter distributions → studied for LHeC and FCC-eh SM Higgs; and for extrapolations [PGS for CDR and until 2014]

- 'Standard' GPD LHC-style detectors used and further studied based on optimising Higgs measurements, i.e. vertex resolution a la ATLAS IBL, excellent hadronic and elmag resolutions using 'best' state-of-the art detector technologies (no R&D 'needed')
- Analysis requirements fed back to ep detector design

* See page 11 for ep Pythia checks
https://indico.cern.ch/event/278903/contributions/631181/attachments/510303/704309/Chavannes_UKLein_20.01.2014.pdf

The Phenomenological Higgs Landscape (Revisited)

Future ep colliders could make important contribution to Higgs physics!

- Mass
- Width (via VV scattering)
- Spin-Parity
- Coupling
  - hVV, hff
  - 3h,4h, hhVV
  - FCNC coupling

- Exotic Higgs Decay
  - h to invisible
  - h to 4b
  - …

➢ Reducing PDF & Alpha_s uncertainties in Higgs measurements

➡ See talk given by Voica Radescu

Philosophy could be traced back to
Phys. Rev. D82 (2010) 016009 by T. Han and B. Mellado.

See also:
M. Kumar et al., 1509.04016
S. S. Biswal et al., Phys. Rev. Lett. 109 (2012) 261801
U. Klein, talk given at LHeC Workshop 2015

Chen Zhan 12.4.16 (talk at annual FCC week 2016, Rome)

BSM: channel h—> sb e. g. Cases in 2HDM-III

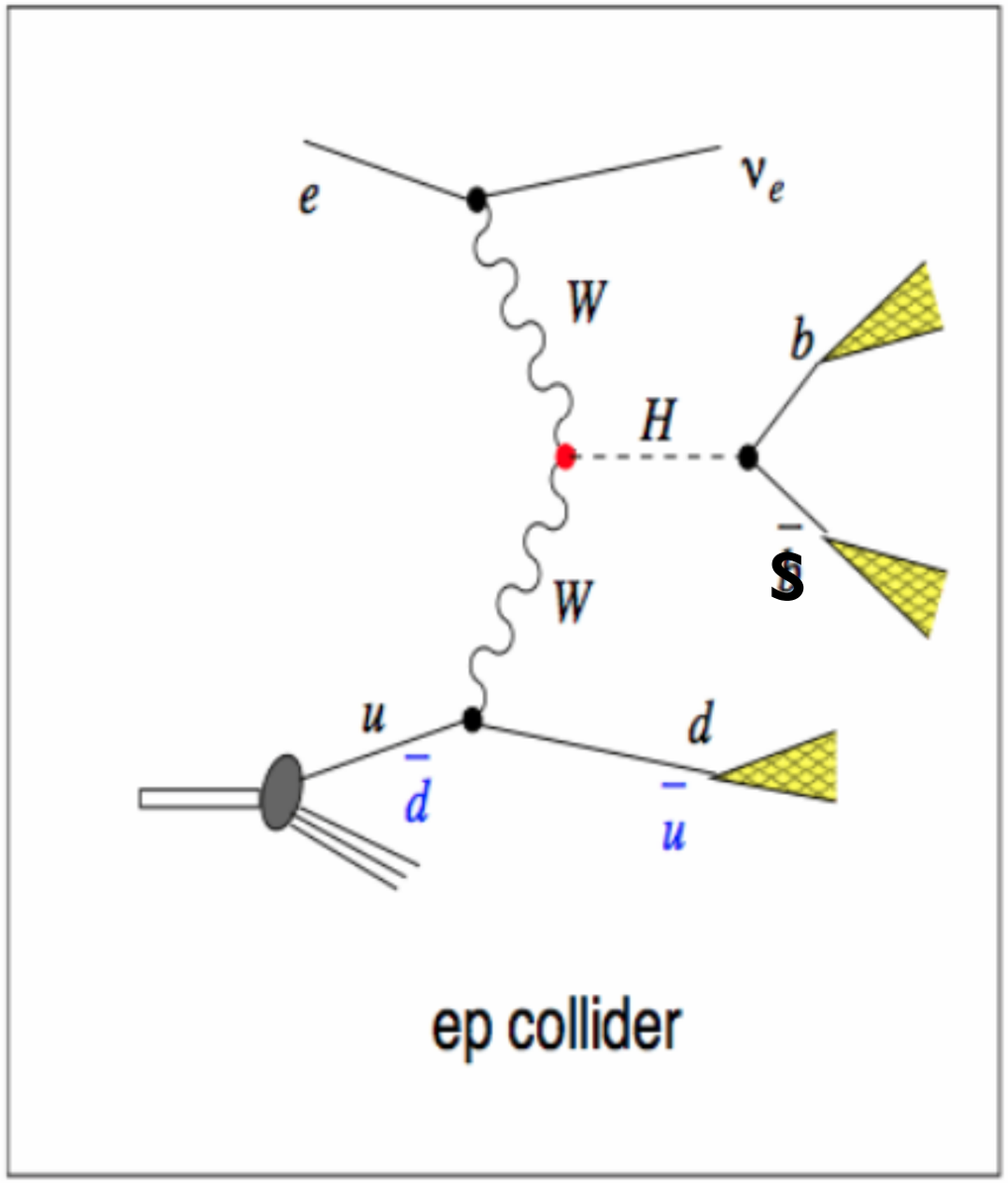

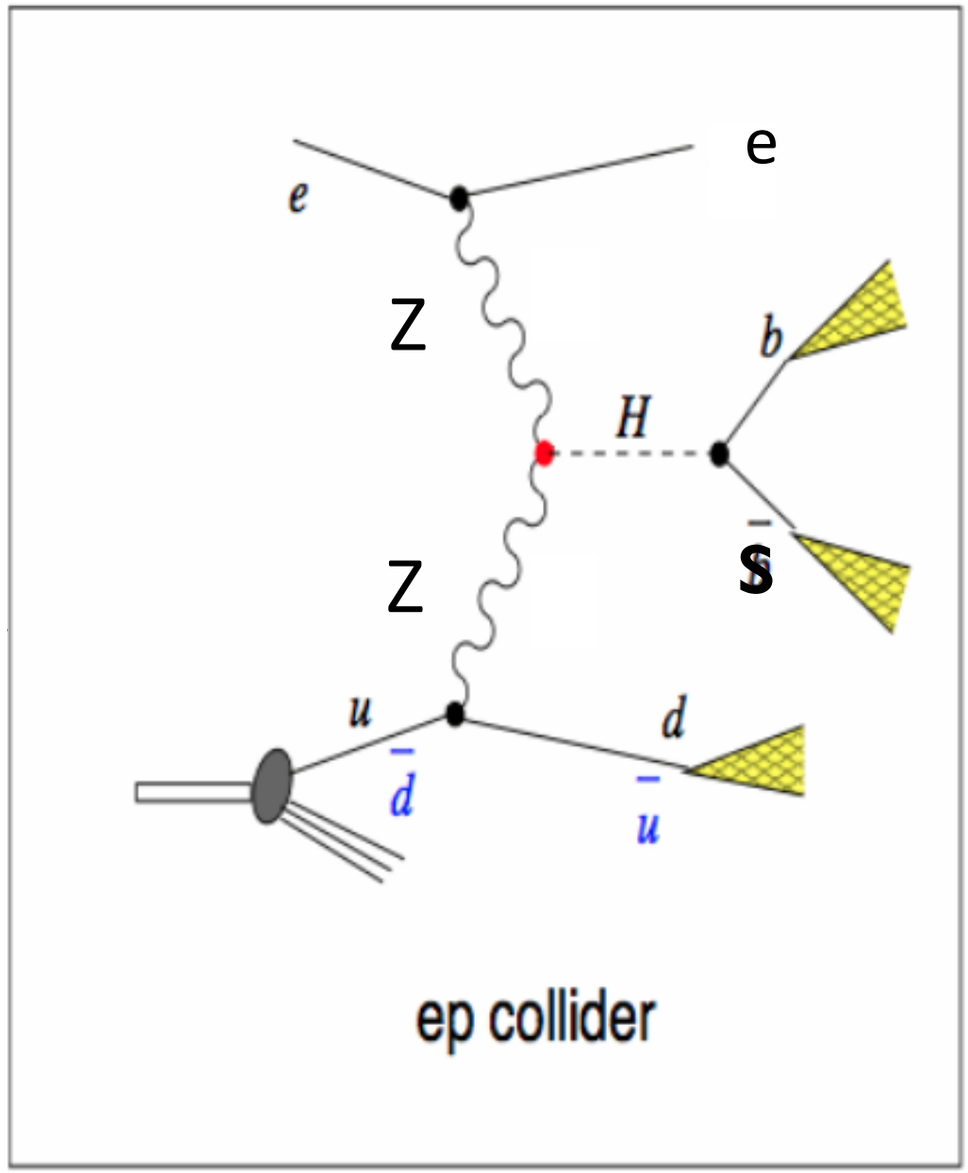

The background is reduced a lot

In the 2HDM; H= h0, H0

For H0 the coupling VVH0 is proportional to Cos(β-α) and VVh0 to Sin(β-α)

Further BSM Higgs Studies

Example: Charged Higgs

- $H\pm$, in Vector Boson Scattering

  [Georges Azuelos, Hao Sun, and Kechen Wang, 1712.07505]

- $H\pm\pm$, in Vector Boson Scattering

  [H. Sun, X. Luo, W. Wei and T. Liu, Phys. Rev. D 96, 095003 (2017)]

- $H+$, in 2HDM type III, $p\ e \rightarrow \nu j H \rightarrow \nu j\ cb$

  [J. Hernández-Sánchez et al., 1612.06316]

Production of H+ in ep collider

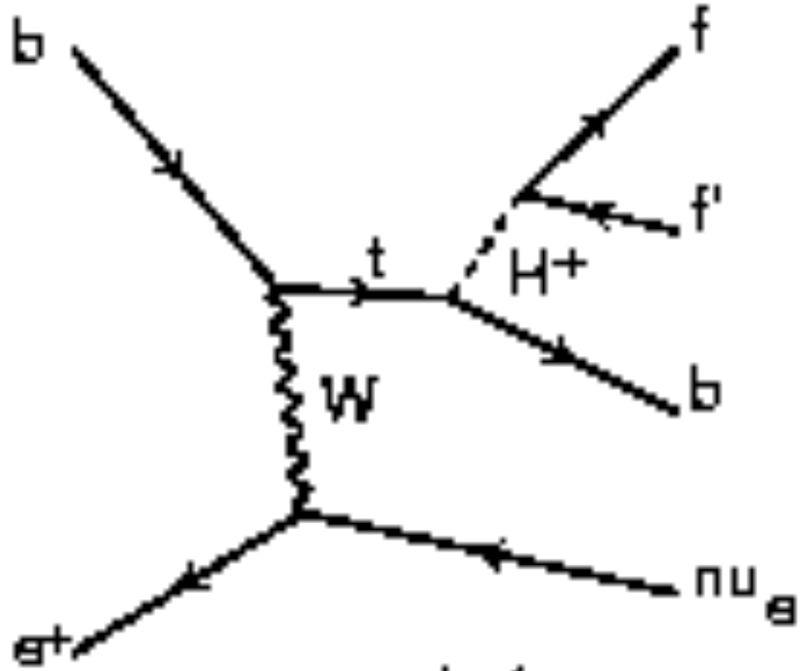

graph 1

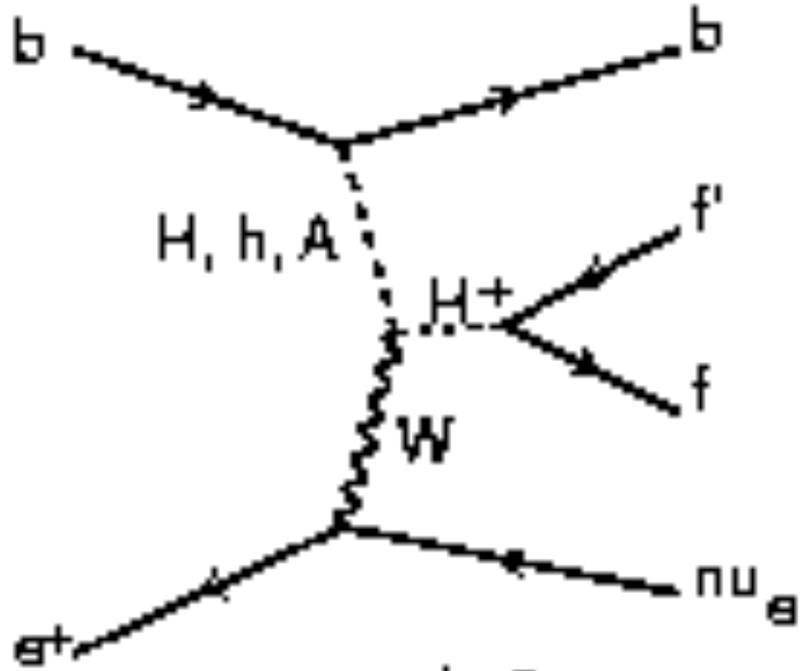

graph 2

We focus in H+ —> cb, in 2HDM-III (also in MHDM) could be relevant

BR (H+ —> cb) ~ 0.9 in 2HDM-III

~0.8 in MHDM (A. Akeroyd, S. Moretti and J. Hernandez-Sanchez, PRD 85, 115002 (2012)) .

BSM: Some arguments o motivations 2HDM-III

The 2HDM-II could be transformed into 2HDM-III through the loops-effects of sfermions and gauginos

Andreas Crivellin, Phys.Rev. D83 (2011) 056001

In models with more than one Higgs doublet the MFV case is more stable in suppressing FCNCs than the hypothesis of NFC when the quantum corrections are taken into account.

A.J. Buras, M.V. Carlucci, S. Gori and G. Isidori, Higgs-mediated FCNCs: Natural Flavour Conservation vs. Minimal Flavour Violation , JHEP 10 (2010) 009 [arXiv:1005.5310].

Similar phenomenology in MHDM with flavor symmetries (Nearest-Neighbor-Interaction texture)

G. C. Branco, L. Lavoura and F. Mota, Phys. Rev. D 39, 3443 (1989)

Alfredo Aranda, Cesar Bonilla, J.Lorenzo Diaz-Cruz. Phys.Lett. B717 (2012) 248-251

2HDMs is studied in renormalization group evolution of the Yukawa couplings and the cases when the Z2-symmetry is broken, called non-diagonal models.

J. Bijnens, J. Lu and J. Rathsman, Constraining General Two Higgs Doublet Models by the Evolution of Yukawa Couplings , JHEP 05 (2012) 118

Yukawa textures in the 2HDM-III

The Yukawa textures are consistents with the relations between quarks masses and flavor mixing parameters.

Yukawa textures could come of a theory more fundamental and it could be a flavor symmetry.

H. Fritzsch, Z. Z. Xing, Prog.Part. Nucl. Phys. 45 (2000)1.
H. Fritzsch, Z. Z. Xing, Phys. Lett. 555 (2003)63.

Yukawa sector in 2HDM type III

$$\mathcal{L}_Y = Y_1^u \bar{Q}_L \Phi_1 u_R + Y_2^u \bar{Q}_L \Phi_2 u_R + Y_1^d \bar{Q}_L \Phi_1 d_R + Y_2^d \bar{Q}_L \Phi_2 d_R \,,$$

$$M_f = \frac{1}{\sqrt{2}}(v_1 Y_1^f + v_2 Y_2^f), \qquad f = u, d, l,$$

$$\bar{M}_f = V_{fL}^{\dagger} M_f V_{fR}.$$

$$M_f = \begin{pmatrix} 0 & C_f & 0 \\ C_f^* & \tilde{B}_f & B_f \\ 0 & B_f^* & A_f \end{pmatrix}.$$

$$(\tilde{Y}_2^l)_{ij} = \frac{\sqrt{m_i m_j}}{v}\tilde{\chi}_{ij} = \frac{\sqrt{m_i m_j}}{v}\chi_{ij} e^{\vartheta_{ij}},$$

The off-diagonal terms are constrained by CKM

F. González, O. Félix-Beltrán, J.Hernandez-Sanchez, S. Moretti, R. Noriega, A. Rosado, Phys.Lett. B742 (2015) 347-352.
J. Hernandez-Sanchez, L. Lopez-Lozano, R. Noriega, A. Rosado, Phys.Rev. D85 (2012) 071301

$$
\begin{aligned}
\mathcal{L}^{\bar{f}_i f_j \phi} \quad = \quad & -\left\{ \frac{\sqrt{2}}{v}\,\overline{u}_i \left(m_{d_j} X_{ij} P_R + m_{u_i} Y_{ij} P_L \right) d_j\, H^+ + \frac{\sqrt{2} m_{l_j}}{v}\, Z_{ij} \overline{\nu_L} l_R H^+ + H.c. \right\} \\
& -\frac{1}{v}\left\{ \bar{f}_i m_{f_i} h^f_{ij} f_j h^0 + \bar{f}_i m_{f_i} H^f_{ij} f_j H^0 - i \bar{f}_i m_{f_i} A^f_{ij} f_j \gamma_5 A^0 \right\},
\end{aligned}
$$

where ϕ^f_{ij} ($\phi = h, H, A$), X_{ij}, Y_{ij} and Z_{ij} are defined as:

$$
\begin{aligned}
\phi^f_{ij} \quad &= \quad \xi^f_\phi \delta_{ij} + G(\xi^f_\phi, X), \quad \phi = h, H, A, \\
X_{ij} \quad &= \quad \sum_{l=1}^{3} (V_{\rm CKM})_{il} \left[X\, \frac{m_{d_l}}{m_{d_j}}\, \delta_{lj} - \frac{f(X)}{\sqrt{2}} \sqrt{\frac{m_{d_l}}{m_{d_j}}}\, \tilde{\chi}^d_{lj} \right], \\
Y_{ij} \quad &= \quad \sum_{l=1}^{3} \left[Y\, \delta_{il} - \frac{f(Y)}{\sqrt{2}} \sqrt{\frac{m_{u_l}}{m_{u_i}}}\, \tilde{\chi}^u_{il} \right] (V_{\rm CKM})_{lj}, \\
Z^l_{ij} \quad &= \quad \left[Z\, \frac{m_{l_i}}{m_{l_j}}\, \delta_{ij} - \frac{f(Z)}{\sqrt{2}} \sqrt{\frac{m_{l_i}}{m_{l_j}}}\, \tilde{\chi}^l_{ij} \right].
\end{aligned}
$$

With this structure in different limits one can have different 2HDM

$$
\left(g^{f_u i f_d j H^+}_{2HDM-III} = g^{f_u i f_d j H^+}_{2HDM-any} + \Delta g^{f_u i f_d j H^+} \right)
$$

J. Hernandez-Sanchez, S. Moretti, R. Noriega-Papaqui, A. Rosado, JHEP07 (2013) 044

2HDM-III	X	Y	Z	ξ_h^u	ξ_h^d	ξ_h^l	ξ_H^u	ξ_H^d	ξ_H^l
2HDM-I-like	$-\cot\beta$	$\cot\beta$	$-\cot\beta$	c_α/s_β	c_α/s_β	c_α/s_β	s_α/s_β	s_α/s_β	s_α/s_β
2HDM-II-like	$\tan\beta$	$\cot\beta$	$\tan\beta$	c_α/s_β	$-s_\alpha/c_\beta$	$-s_\alpha/c_\beta$	s_α/s_β	c_α/c_β	c_α/c_β
2HDM-X-like	$-\cot\beta$	$\cot\beta$	$\tan\beta$	c_α/s_β	c_α/s_β	$-s_\alpha/c_\beta$	s_α/s_β	s_α/s_β	c_α/c_β
2HDM-Y-like	$\tan\beta$	$\cot\beta$	$-\cot\beta$	c_α/s_β	$-s_\alpha/c_\beta$	c_α/s_β	s_α/s_β	c_α/c_β	s_α/s_β

- $\mu - e$ universality in τ decays
- Leptonic meson decays $B \to \tau\nu$, $D \to \mu\nu$, $D_s \to \mu\nu, \tau\nu$ and semileptonic decays $B \to D\tau\nu$
- $B \to X_s\gamma$ decays
- $B^0 - \bar{B}^0$ mixing
- Eelectro-weak precision test(including S,T,U oblique parameters)

Finally with all these above constraints one can find: $\chi^f_{kk} \sim 1$ and $|\chi^f_{ij}| \leq 0.5$,

The 2HDM-III as effective Lagrangian that induce at tree level flavor violating signatures like h,H —> sb, τμ and H+ —> cb, ts, decays can be relevant in the parameter space of the model.

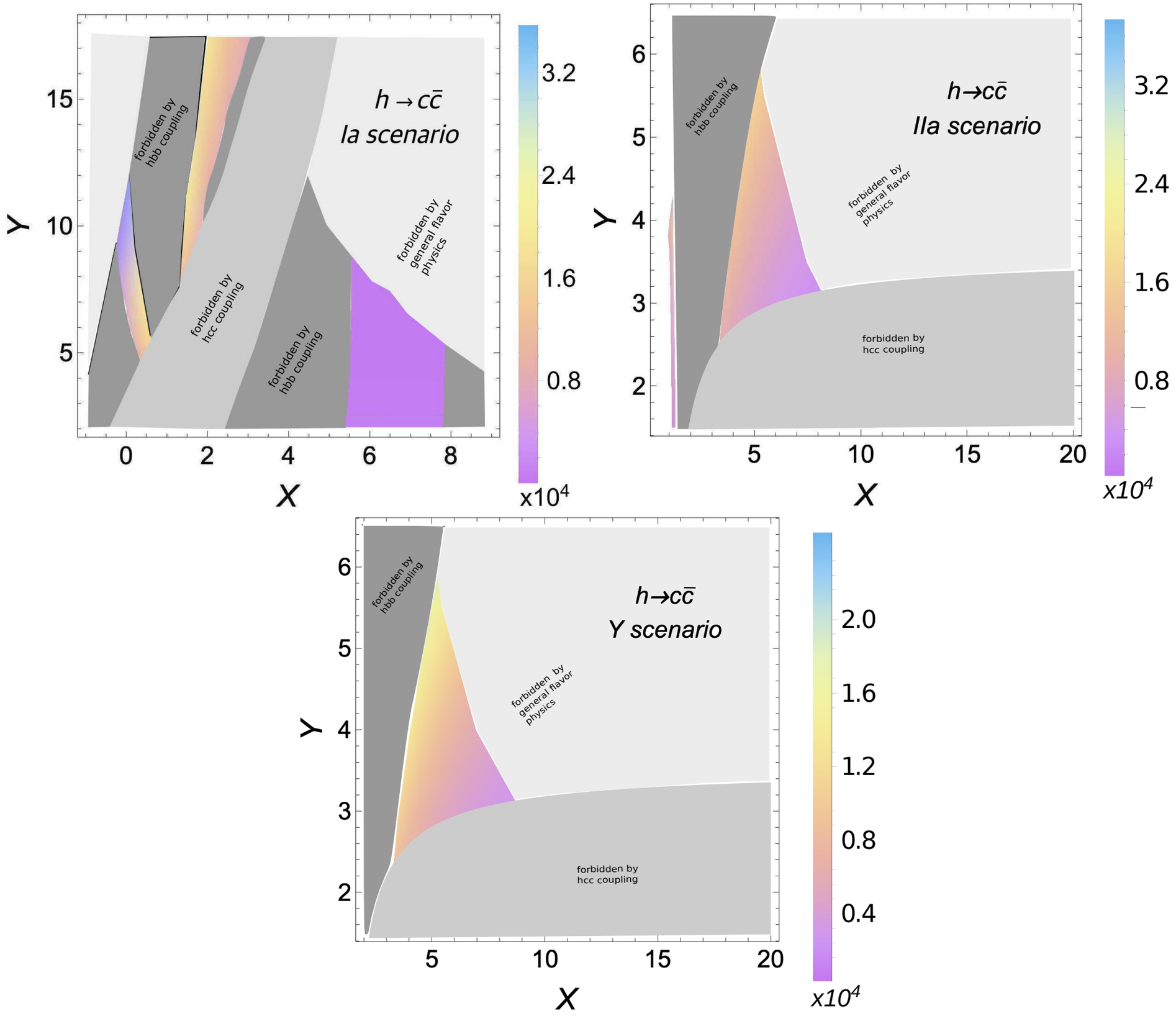

FIG. 1. Event rates for each benchmark scenario over the (X, Y) plane computed as $\sigma(ep \to \nu_e hj) \times \mathrm{BR}(h \to c\bar{c}) \times \epsilon_c^2 \times 1\ \mathrm{ab}^{-1}$. Here, we have $E_p = 50$ TeV and $E_{e^-} = 60$ GeV (with $P_L^{e^-} = -80\%$).

Limits for masses of neutral Higgs bosons:

An additional state with the same mass of the Higgs boson of SM is not ruled out, in particular the 2HDM-I could render it [arXiv:1307.1347 [hep-ph]].

CMS Collaboration analyse the range 110 GeV< M_H < 150 GeV in the almost case degenerate for the masses of Higgs boson, which is not excluded yet.

This result can be employed for CP-odd state.

Recently for CP-odd sate in any 2HDM, CMS has ruled out the range 225 GeV< m_A < 1000 GeV, considering low values of tan β [A. M. Sirunyan et al. (CMS), Eur. Phys. J. C 79, 564 (2019), arXiv:1903.00941 [hep-ex]].

Limits for masses of charged Higgs bosons:

CMS and ATLAS Collab-oration has imposed for the range of the mass 80 GeV < $m_{H^\pm}$ < 160 GeV, a higher limit for BR(t H^+b) = 2 – 3%, assuming BR($H^+ \rightarrow \tau + \nu$) = 1 [V. Khachatryan et al. (CMS), JHEP 11, 018 (2015), arXiv:1508.07774 [hep-ex]],[M. Aaboud et al. (ATLAS), JHEP 09, 139 (2018), arXiv:1807.07915 [hep-ex]].

On the other hand, when BR($H^+ \rightarrow c\bar{s}$) = 1 is assumed, CMS collaboration establish BR(t → H^+b)~20%in the mass range 90GeV<$m_{H^\pm}$ <160 GeV [V.Khacha- tryan et al. (CMS), JHEP 12, 178 (2015), arXiv:1510.04252 [hep-ex]], [A. M. Sirunyan et al. (CMS), Phys. Rev. D 102, 072001 (2020), arXiv:2005.08900 [hep-ex]].

Besides, for the case BR($H^+ \rightarrow c\bar{b}$) = 1 and in the mass range 90GeV<$m_{H^\pm}$<160GeV, CMS give us a limit for BR(t H^+b) ~ 0.5 – 0.8% [A. M. Sirunyan et al. (CMS), JHEP 11, 115 (2018), arXiv:1808.06575 [hep-ex]].

Lastly, very recently ATLAS collaboration has reported limits for the product of branching fractions BR(t H^+b) × BR($H^+ \rightarrow c\bar{b}$) = 0.15% – 0.42% in the mass range 60 GeV < $m_{H^\pm}$ < 160 GeV, also reporting a slight excess in $m_{H^\pm}$ = 130 GeV [Collaboration (ATLAS), ATLAS-CONF-2021-037 (2021)].

Process: $e^- p \to \nu_e \phi q_f$; $\phi \to b\bar{s}$ +h.c.

These processes lead to 3-jets+ $\not{E}_T$

We demanded two jets in the central rapidity region: one tagged b-jet and one low flavor jet.

The remaining jet (q_f) has been tagged in the forwards region and the central jet veto (no more than one low flavor jet): are criterions to enhance the signal to the SM backgrounds.

TABLE I. Parameters for few optimistic benchmark points in the 2HDM-III as a 2HDM-I, -II and -Y configuration. Here bs stands for $\mathrm{BR}(\phi \to b\bar{s} + \bar{b}s)$, in units of 10^{-2}, where $\phi = h, H$, while $\sigma.bs$ stands for the cross section multiplied by the above BR as obtained at the LHeC in units of fb. We have analyzed only the benchmarks where the $\sigma.bs$ is greater than 0.15 fb, so that at least 15 events are produced for 100 fb^{-1}.

				$m_h = 125$ GeV		$m_H = 130$ GeV		$m_H = 150$ GeV		$m_H = 170$ GeV	
2HDM	X	Y	Z	bs	$\sigma.bs$	bs	$\sigma.bs$	bs	$\sigma.bs$	bs	$\sigma.bs$
Ib35	28	10	28	15.66	6.392	51.8	1.209	51.6	0.30	1.58	0.117
Ib47	30	5	30	16.14	3.086	48.2	10.983	48.0	0.127	1.80	0.839
Ib57	44	5	44	17.58	11.861	38.6	5.14	38.4	2.303	3.68	0.137
IIa11	20	2	20	1.42	1.055	25.2	0.097	25.0	0.091	24.8	0.085
IIa14	26	2	26	1.44	1.651	26.0	0.059	25.8	0.054	25.6	0.049
IIa26	36	1	36	1.46	1.621	26.4	0.045	26.2	0.042	26.0	0.038
Ya11	20	2	−2	1.42	1.084	25.2	0.062	25.0	0.059	24.8	0.054
Ya12	22	2	−2	1.44	1.078	25.6	0.057	25.4	0.053	25.2	0.048
Ya14	26	2	−2	1.46	1.441	26.0	0.057	25.8	0.053	25.6	0.049

We consider only σ.bs > 0.15 fb; at least 15 events for 100 fb^(-1)

We applied the following basic preselections:

$$p_T^q > 15.0 \quad \mathrm{GeV}, \Delta R(q,q) > 0.4$$

$\Delta R = \Delta\eta^2 + \Delta\phi^2$, where η and ϕ are the pseudo-rapidity and azimuthal angle respectively.

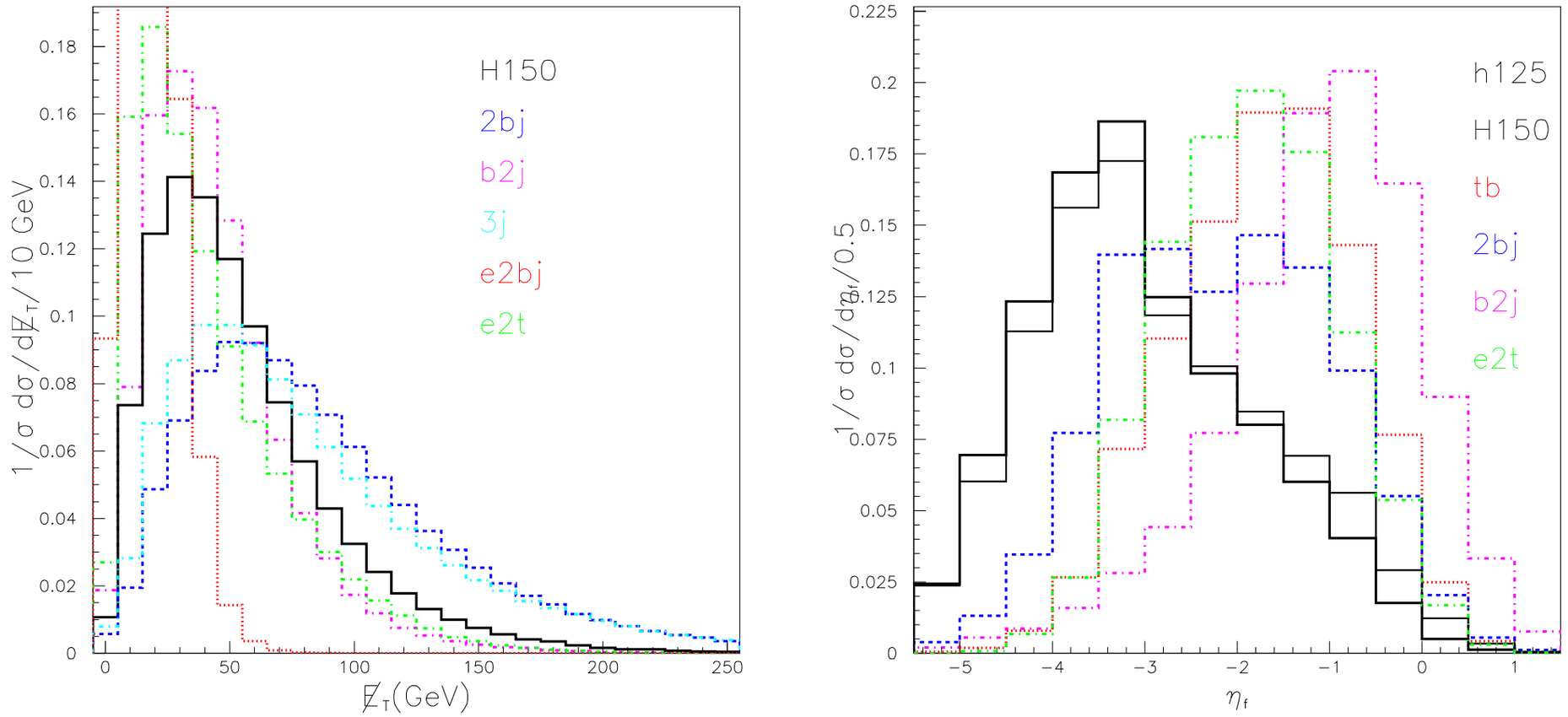

FIG. 9. The missing energy ($\not\!\!E_T$) (left panel) and rapidity (η_{j_f}) (right panel) profile of the forward jet for signals and SM backgrounds. The $\not\!\!E_T$ distributions for all other signal benchmarks as well as the $t\bar{b}$ noise are not shown as they are very similar to the signal distributions of m_H=150 GeV for Scenario Ib with $X = Z = 28$ and $Y = 10$ (shown in thick solid), whereas the thin solid is for m_h=125 GeV for Scenario Ia with $X = Z = 28$ with $Y = 10$. The rapidity distributions profile for m_H=130(170) GeV is very close to the m_h=125 GeV(m_H=130 GeV) case shown in thin solid, except that for massive Higgs the peaks shift towards the left. Also the corresponding rapidity distribution profile for *e2bj* is somewhat similar to the m_h=125 GeV signal case.

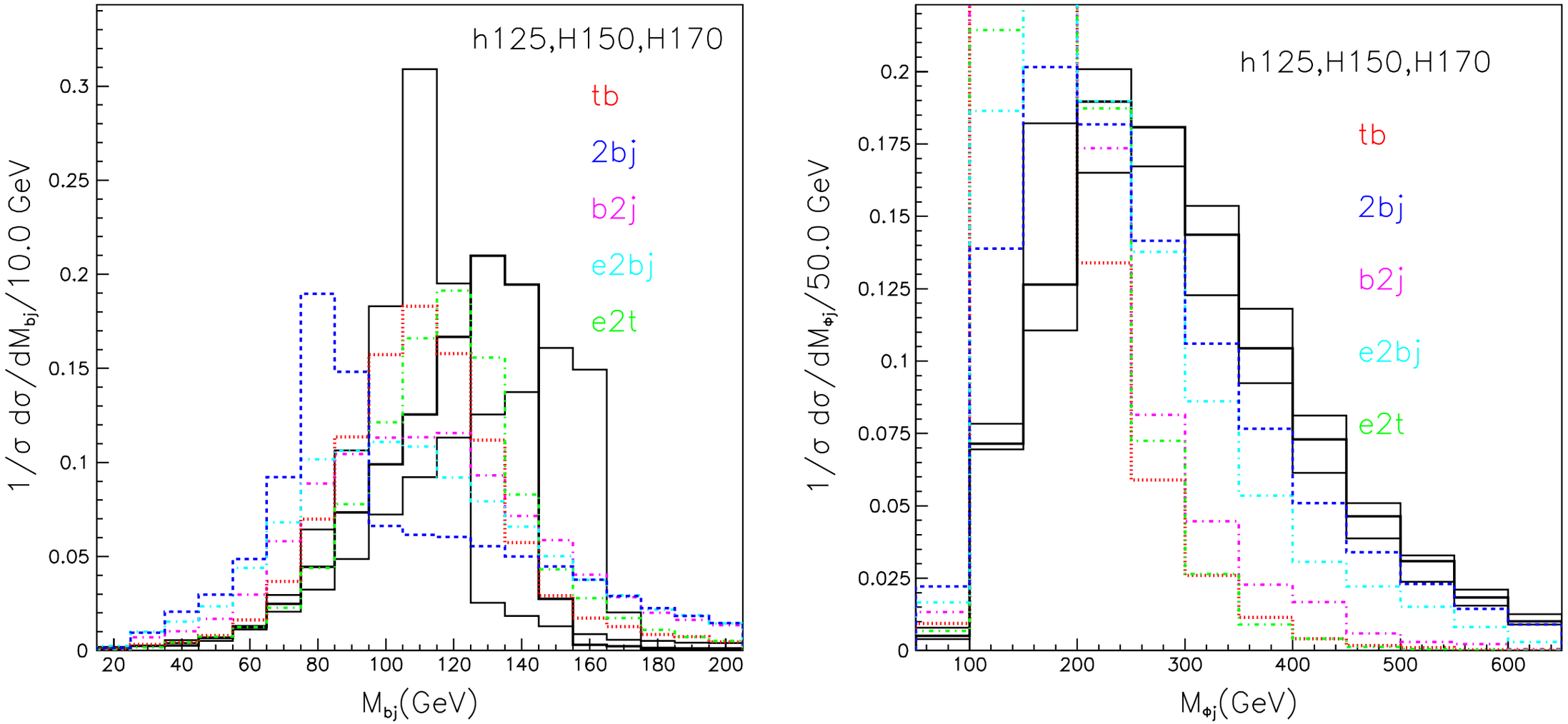

FIG. 6. The dijet invariant mass, made up by one b-tagged and one light-flavor jet, producing Higgs candidates, $M_\phi = M_{bj}$ (left panel) and the three-jet invariant mass, i.e., the previous two jets combined together with the forward jet, $M_{\phi j_f}$ (right panel). The mass peaks of the Higgs signals (M_ϕ) correspond to $m_h = 125$ (thin black) for Scenario Ia, $m_H = 150$ (thick black) and 170 (thin black) for Scenario Ib from left to right. All these are using the parameters $X = Z = 28$ and $Y = 10$. The distribution for $m_H = 130$ is not shown but it lies in between $m_h = 125$ and $m_H = 150$. Among all SM backgrounds, only $2bj$ shows a prominent peak from the Z-boson. Notice that $M_{\phi j_f}$ represents the overall energy scale of the hard-scattering.

h_{SM}=125 GeV:3-jet+$\not{E}_T$ with 100 fb^{-1}

- a: $N_j \gtrsim 3$
- b: $N_{b-tag} \gtrsim$ 1 (with ϵ_b=0.50, ϵ_c=0.10 and ϵ_j=0.01, where j=u,d,s,g)
- cd : at least two central jets (within $\eta < 2.5$) with $\not{E}_T > 20 GeV$ → 3j not survive and photo production is reduced
- e: lepton (e or μ) veto with $p_T > 20$ GeV and $\eta < 3.0$
- f: in the central region: $|M_{bj} - M_{h(H)}|$ is minimum and with 15 GeV mass windows.
- g: remaining leading jet with $p_T > 25$ GeV and $-5.5 < \eta < -0.5$
- h: $m_{\phi j_f} > 190$ GeV

i:We required only one low flavored jet in the central regions (this has severe impact on the processes)

Details in arXiv: 1503.01464
PRD 94, 055003 (2016)

- S.P. Das, J. Hernández-Sánchez, S. Moretti, A. Rosado, R. Xoxocotzi

TABLE II. Expected number of events after different combinations of cuts for signal and backgrounds at the LHeC with an integrated luminosity of 100 fb^{-1} for $m_h = 125$ GeV. SimEvt stands for the actual number of events analyzed in the Monte Carlo simulations. RawEvt stands for the number of events with only the generator–level cuts (14) imposed; for the signal as well as for background, these are calculated from the total cross section times branching ratio. In the final column we mention the significances($\mathcal{S}$) defined as $\mathcal{S} = S/\sqrt{B}$, where S stands for signal events, background events B for 100 fb^{-1} of data after all cuts mentioned in the "i" column. The number in the parenthesis in the final column represent the significances for 1000 fb^{-1}.

Proc	SimEvt	RawEvt	a	b	c	d	e	f	g	h	i	$\mathcal{S}$
Ib35	100 K	639.2	447.6	177.3	117.1	97.4	93.8	37.8	31.7	25.4	15.8	1.2(3.8)
Ib47	100 K	308.6	216.8	85.1	56.2	47.1	45.5	18.4	15.6	13.0	8.1	0.62(2.0)
Ib57	100 K	1186.1	833.7	325.7	215.5	180.6	173.9	70.3	59.1	49.3	31.1	2.4(7.5)
IIa11	100 K	105.5	74.3	29.1	19.2	16.0	15.4	6.3	5.3	4.4	2.8	0.21(0.70)
IIa14	100 K	165.1	116.1	45.2	30.0	25.4	24.4	9.7	8.3	6.9	4.4	0.33(1.05)
IIa26	100 K	162.1	114.4	44.7	29.5	24.5	23.6	9.5	8.1	6.8	4.3	0.33(1.03)
Ya11	100 K	108.4	76.3	29.8	19.6	16.4	15.8	6.4	5.4	4.6	2.9	0.22(0.70)
Ya12	100 K	107.8	76.2	29.6	19.5	16.3	15.7	6.3	5.4	4.5	2.8	0.21(0.67)
Ya14	100 K	144.1	101.7	39.8	26.0	21.7	20.8	8.2	7.0	5.9	3.8	0.29(0.92)
$\nu t\bar{b}$	100 K	50712.1	28338.4	15293.7	9845.0	8144.2	7532.7	2982.1	2058.0	652.2	139.6	
$\nu b\bar{b}j$	560 K	14104.6	6122.8	3656.7	1858.5	1787.1	1650.1	257.5	152.5	85.2	15.1	
$\nu b2j$	90 K	18043.1	8389.2	3013.0	1691.5	1445.5	1373.7	389.5	206.1	77.2	11.3	$B = 170.8$
$\nu 3j$	300 K	948064.2	410393.4	15560.9	0.0	0.0	0.0	0.0	0.0	0.0	0.0	$\sqrt{B} = 13.1$
$eb\bar{b}j$	115 K	256730.1	55099.8	36353.6	12659.8	1432.0	200.7	54.1	24.8	18.0	4.5	
$et\bar{t}$	130 K	783.3	685.0	384.5	265.9	179.3	26.2	11.6	10.5	3.9	0.3	

TABLE III. Same as Table II but for $m_H = 130$ GeV. The criterion for jets and b-tagging are the same, so that the number of events in column A and B are the same for all SM backgrounds.

Proc	SimEvt	RawEvt	A	B	C	D	E	F	G	H	I	$\mathcal{S}$
Ib35	100 K	120.9	87.1	34.1	26.9	22.5	21.6	7.5	6.1	5.3	3.4	0.28(0.88)
Ib47	100 K	1098.3	790.3	307.1	243.9	204.6	195.7	68.5	56.1	48.6	31.3	2.6(8.1)
Ib57	100 K	514.0	371.2	144.8	115.0	96.0	92.0	31.7	25.8	22.7	14.3	1.2(3.7)
IIa11	100 K	9.7	6.8	2.7	2.1	1.8	1.7	0.6	0.4	0.3	0.2	0.02(0.05)
IIa14	100 K	5.9	4.2	1.7	1.3	1.1	1.0	0.4	0.3	0.2	0.1	0.01(0.02)
IIa26	100 K	4.5	3.1	1.3	1.0	0.8	0.8	0.3	0.2	0.1	0.1	0.01(0.02)
Ya11	100 K	6.2	4.4	1.8	1.4	1.1	1.1	0.4	0.3	0.2	0.1	0.01(0.02)
Ya12	100 K	5.7	4.0	1.6	1.3	1.0	1.0	0.3	0.2	0.2	0.1	0.01(0.02)
Ya14	100 K	5.7	4.0	1.6	1.3	1.0	1.0	0.3	0.2	0.2	0.1	0.01(0.02)
$\nu t\bar{b}$	100 K	50712.1	28338.4	15293.7	10976.4	9092.4	8393.6	2550.9	1565.5	617.9	113.7	
$\nu b\bar{b}j$	560 K	14104.6	6122.8	3656.7	2145.5	2062.1	1902.9	266.6	141.0	87.5	14.4	
$\nu b2j$	90 K	18043.1	8389.2	3013.0	2053.6	1734.0	1650.1	402.8	143.7	64.5	8.1	$B = 147.8$
$\nu 3j$	300 K	948064.2	410393.4	15560.9	0.0	0.0	0.0	0.0	0.0	0.0	0.0	$\sqrt{B} = 12.2$
$eb\bar{b}j$	115 K	256730.1	55099.8	36353.6	16838.4	1826.6	284.1	56.4	31.6	22.6	11.3	
$et\bar{t}$	130 K	783.3	685.0	384.5	280.8	190.8	27.8	10.9	9.3	3.9	0.3	

Production of H- in ep collider

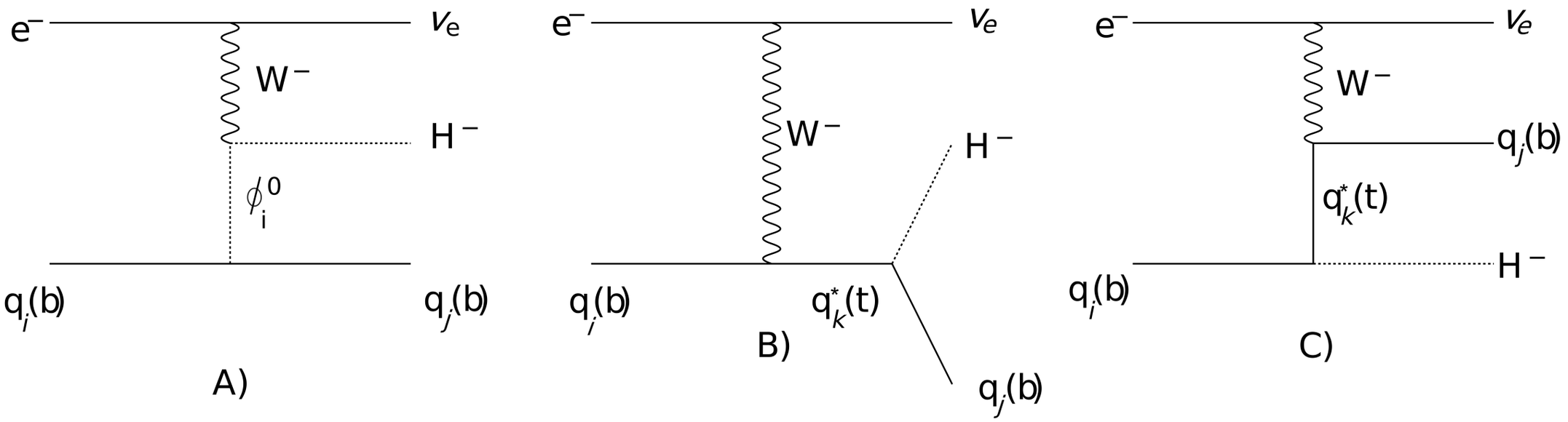

FIG. 1. Feynman diagrams for the $e^-\ p \to \nu_e H^- q$ process. Here, $\phi_i^0 = h, H, A$, i.e., any of the neutral Higgs bosons of the BSM scenario considered here (see below).

J. Hernandez-Sanchez, C.G. Honorato, S. Rosado, S. Moretti,
Phys.Rev.D 99 (2019) 9, 095009

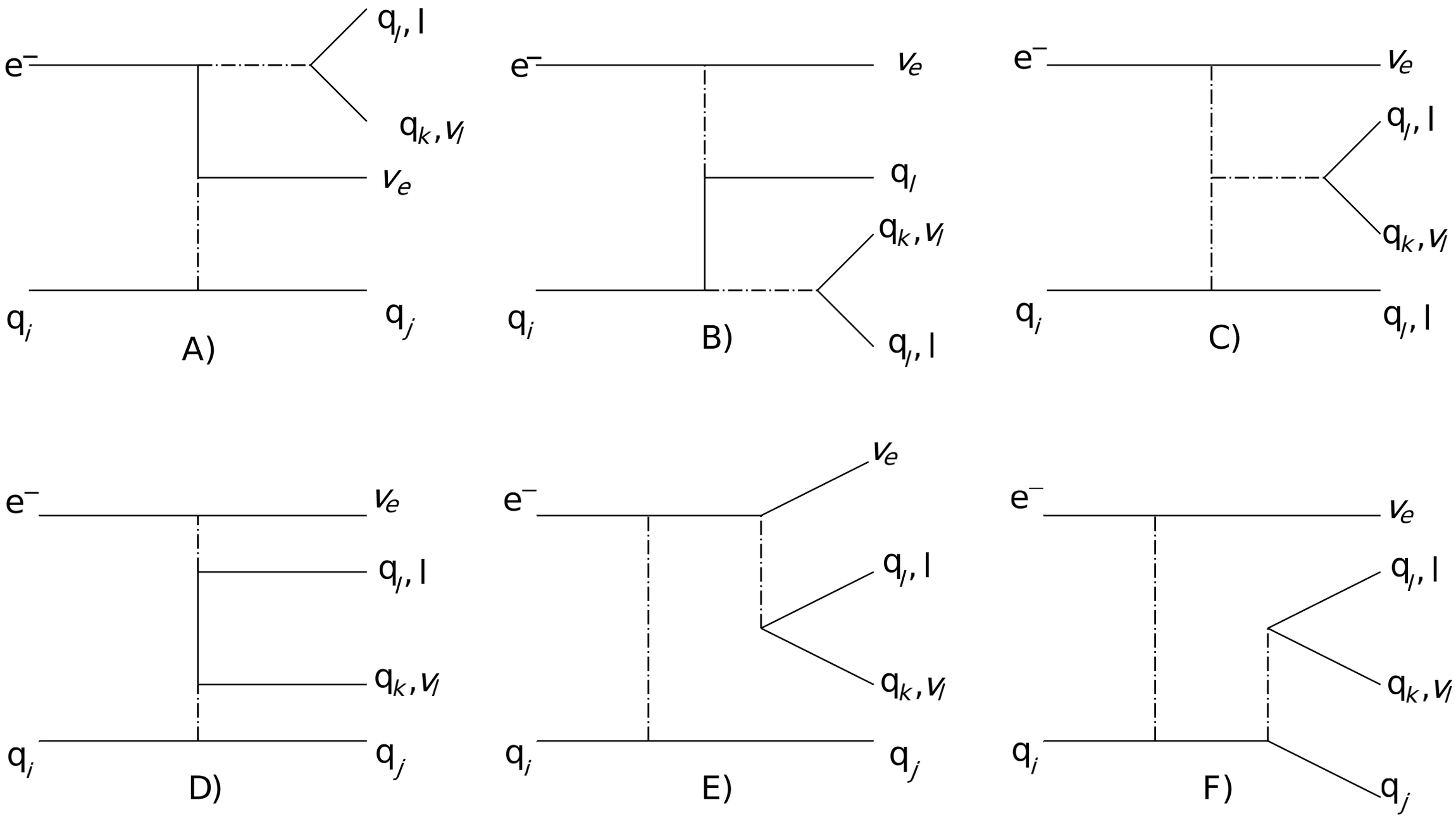

FIG. 2. Feynman diagrams for the $\nu_e jjj$, $\nu_e bjj$ and $\nu_e bbj$ backgrounds (the change $q_l \leftrightarrow l$ and $q_k \leftrightarrow \nu_l$ represents the $\nu_e \nu_l lj$ and $\nu_e \nu_l lb$ backgrounds). Dash-dot lines represent boson fields: (pseudo)scalars and EW gauge bosons.

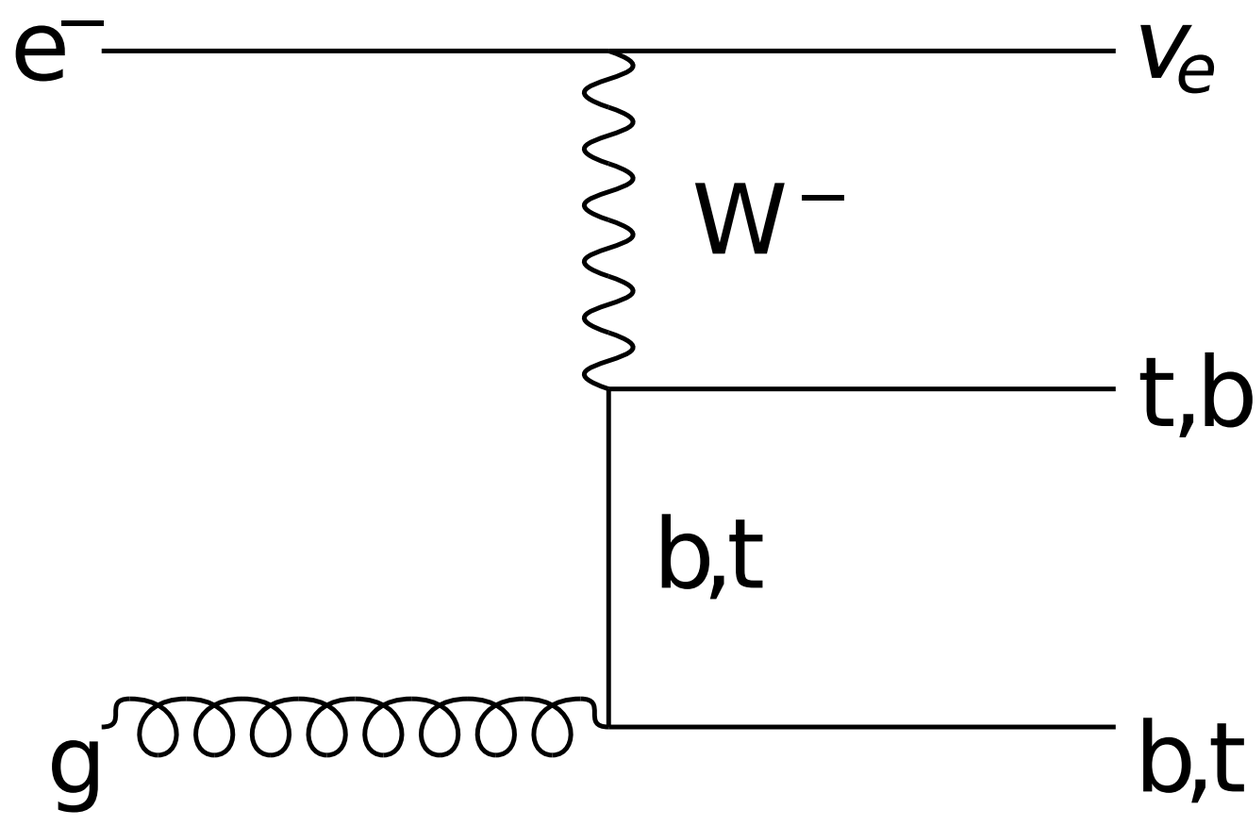

FIG. 3. Feynman diagrams for the $\nu_e bt$ background.

Benchmarks points of 2HDM-III for analysis of H+

2HDM-III	Parameters			$\sigma(ep \to \nu_e H^- q)$ (pb)				BR($H^- \to b\bar{c}$)	BR($H^- \to \tau\bar{\nu}_\tau$)
like-	X	Y	Z	$m_{H^\pm} = 110$ GeV	130 GeV	150 GeV	170 GeV	$m_{H^\pm} = 110$ GeV	$m_{H^\pm} = 110$ GeV
I	0.5	17.5	0.5	2.56×10^{-2}	1.30×10^{-2}	3.47×10^{-3}	1.35×10^{-4}	9.57×10^{-1}	2.5×10^{-4}
II	20	1.5	20	2.18×10^{-2}	1.13×10^{-2}	2.95×10^{-3}	5.89×10^{-5}	9.9×10^{-1}	2.22×10^{-4}
X	0.03	1.5	-33.33	6.49×10^{-2}	3.39×10^{-2}	8.83×10^{-3}	2.34×10^{-4}	9.28×10^{-2}	9.04×10^{-1}
Y	13	1.5	$-1/13$	6.41×10^{-2}	3.27×10^{-2}	8.47×10^{-3}	2.2×10^{-4}	9.91×10^{-1}	6.12×10^{-3}

TABLE II. The BPs that we studied for the 2HDM-III in the incarnations like-I, -II, -X and -Y. We present cross sections and BRs at Parton level, for some $H^\pm$ mass choices.

- Scenario 2HDM-III like-I: $\cos(\beta-\alpha) = 0.5$, $\chi^u_{22} = 1$, $\chi^u_{23} = 0.1$, $\chi^u_{33} = 1.4$, $\chi^d_{22} = 1.8$, $\chi^d_{23} = 0.1$, $\chi^d_{33} = 1.2$, $\chi^\ell_{22} = -0.4, \chi^\ell_{23} = 0.1$, $\chi^\ell_{33} = 1$ with $Y \gg X$, Z.

- Scenario 2HDM-III like-II: $\cos(\beta-\alpha) = 0.1$, $\chi^u_{22} = 1$, $\chi^u_{23} = -0.53$, $\chi^u_{33} = 1.4$, $\chi^d_{22} = 1.8$, $\chi^d_{23} = 0.2$, $\chi^d_{33} = 1.3$, $\chi^\ell_{22} = -0.4, \chi^\ell_{23} = 0.1$, $\chi^\ell_{33} = 1$ with X, $Z \gg Y$.

- Scenario 2HDM-III like-X: the same parameters of scenario 2HDM-III like-II but $Z \gg X$, Y.

- Scenario 2HDM-III like-Y: the same parameters of scenario 2HDM-III like-II but $X \gg Y$, Z.

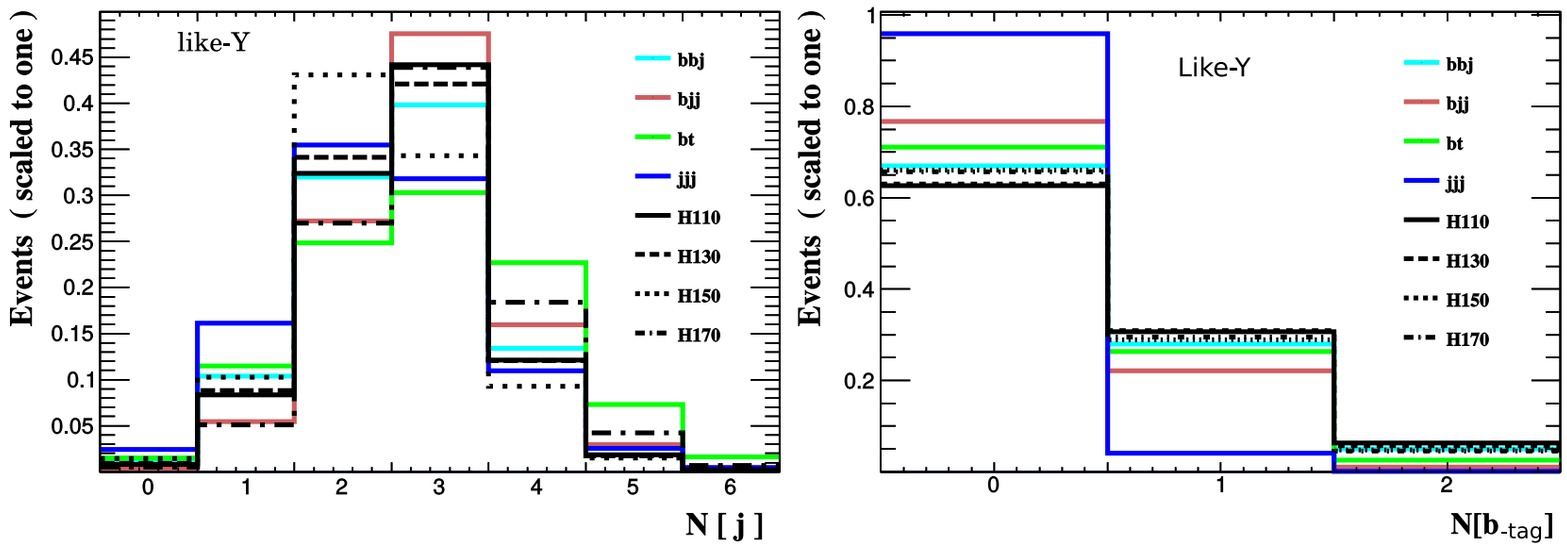

FIG. 6. Distributions for the process $e^- q \to \nu_e H^- b$ followed by $H^- \to b\bar{c}$: in the left panel we present the multiplicity of all jets while in the right panel we present the multiplicity of the b-tagged ones. The like-Y case is illustrated. The normalisation is to unity.

Cut 1: Select 3 jets

Cut 2: Select 2 jet b-tagged for
H - —>cb
1 jet b-tagged for H- —>tau nu

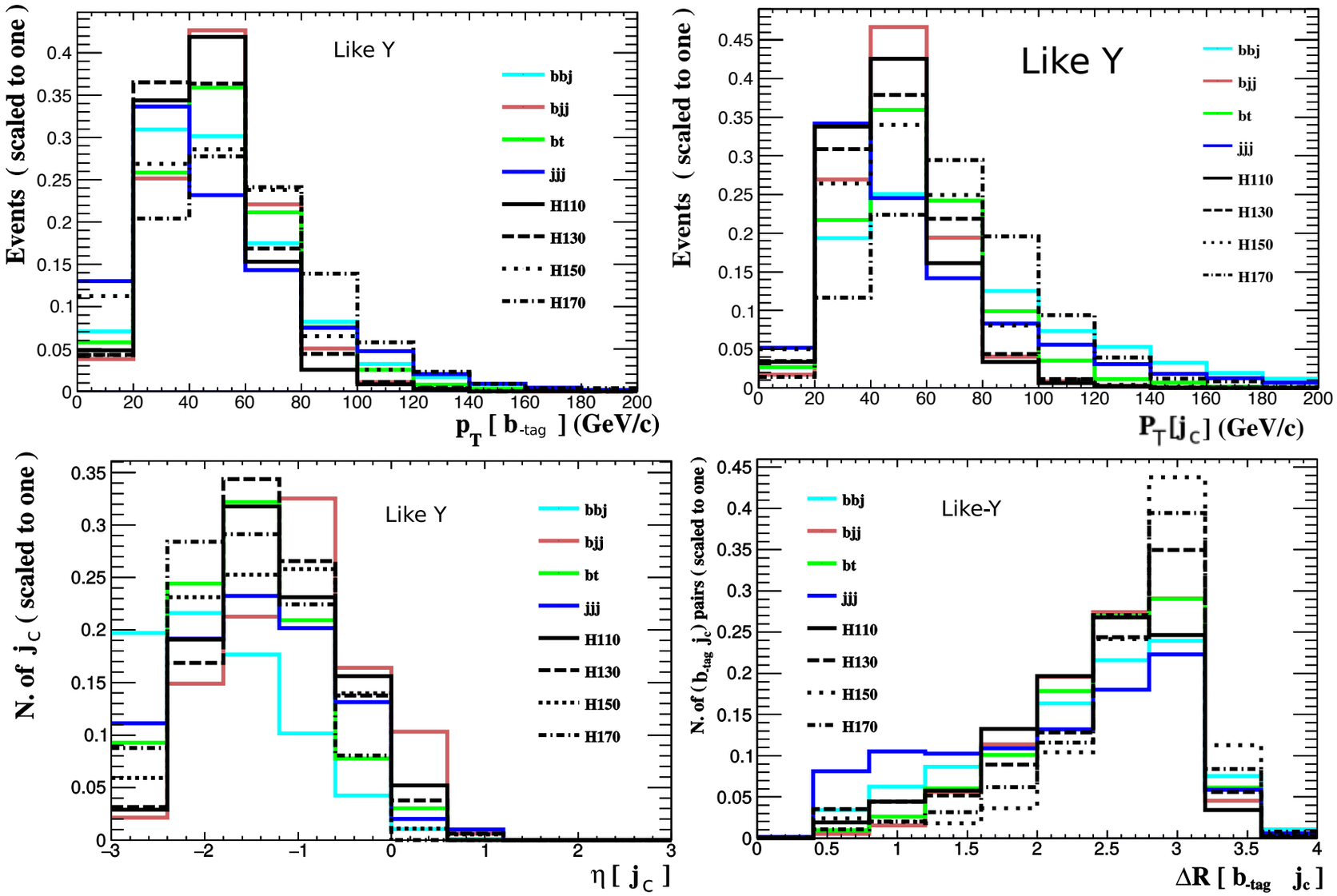

FIG. 7. Distributions for the process $e^- q \to \nu_e H^- b$ followed by $H^- \to b\bar{c}$: in the top-left panel we present the transverse momentum of the central b-tagged jet, in the top-right panel we present the transverse momentum of the central light jet, in the bottom-left panel we present the pseudorapidity of the central light jet while in the bottom-right panel we present the separation between the two central jets. The like-Y case is illustrated. The normalisation is to unity.

Cut 3: PT > 30 GeV. Cut 4 : eta<|2.5|

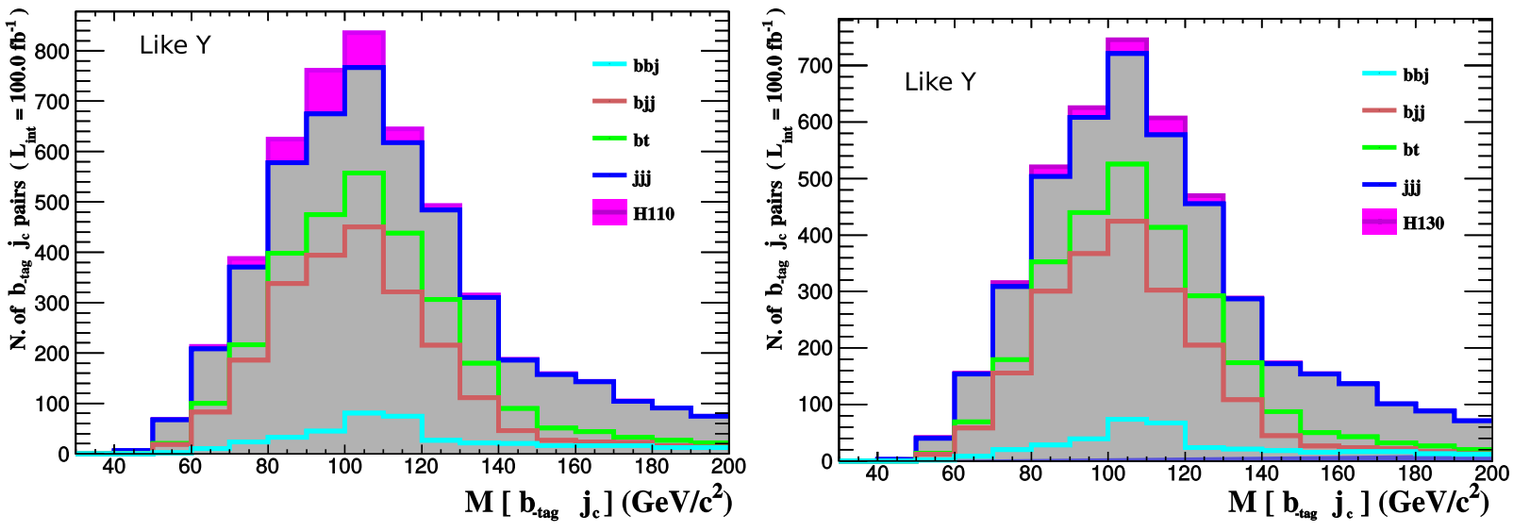

FIG. 8. Distributions for the process $e^- q \to \nu_e H^- b$ followed by $H^- \to b\bar{c}$ in the invariant mass of the two central jets for $m_{H^\pm} = 110$ GeV (left) and $m_{H^\pm} = 130$ GeV (right). The like-Y case is illustrated. The normalisation is to the total event rate for $L = 100$ fb^{-1}.

Signal	Scenario	Events (raw)	Cut I	Cut II	Cut III	Cut IV	$(\mathcal{S}/\sqrt{\mathcal{B}})_{100\,\text{fb}^{-1}(1000\,\text{fb}^{-1})[3000\,\text{fb}^{-1}]}$
$\nu_e H^{\pm} b$	I-110	2562	298	182	134	54	1.43 (4.52) [7.82]
	I-130	1300	139	82	64	19	0.58 (1.82) [3.16]
	I-150	347	29	13	11	3	0.16 (0.5) [0.86]
	I-170	13	1.29	0.62	0.51	0.14	0.01 (0.03) [0.05]
$\nu_e H^{\pm} b$	II-110	2183	245	151	122	53	1.4 (4.43) [7.68]
	II-130	1128	128	84	71	22	0.7 (2.21) [3.82]
	II-150	294	28	14	13	4	0.2 (0.65) [1.13]
	II-170	6	0.6	0.33	0.3	0.08	0.005 (0.017) [0.029]
$\nu_e H^{\pm} b$	Y-110	6417	468	567	347	156	4.18 (12.99) [22.5]
	Y-130	3268	366	204	156	46	1.43 (4.53) [7.84]
	Y-150	847	68	29	23	6	0.33 (1.06) [1.83]
	Y-170	22	2.3	1.12	0.89	0.25	0.017 (0.05) [0.09]
$\nu_e bbj$		20169	2011	748	569	125	$\mathcal{B} = 1441$ $\sqrt{\mathcal{B}} = 37.9$
$\nu_e bjj$		117560	10278	7211	5011	718	
$\nu_e bt$		41885	2278	1418	1130	188	
$\nu_e jjj$		867000	9238	3221	2593	409	

TABLE III. Significances obtained after the sequential cuts described in the text for the signal process $e^- q \to \nu_e H^- b$ followed by $H^- \to b\bar{c}$ for four BPs in the 2HDM-III like-I, -II and -Y. The simulation is done at detector level. In the column Scenario, the label A-110(130)[150]{170} means $m_{H^\pm} = 110(130)[150]\{170\}$ GeV in the 2HDM-III like-A, where A can be I, II and Y.

The process $e^- q \to \nu_e H^- b$ with $H^- \to \tau \bar{\nu}_\tau$ in the 2HDM-III like-X

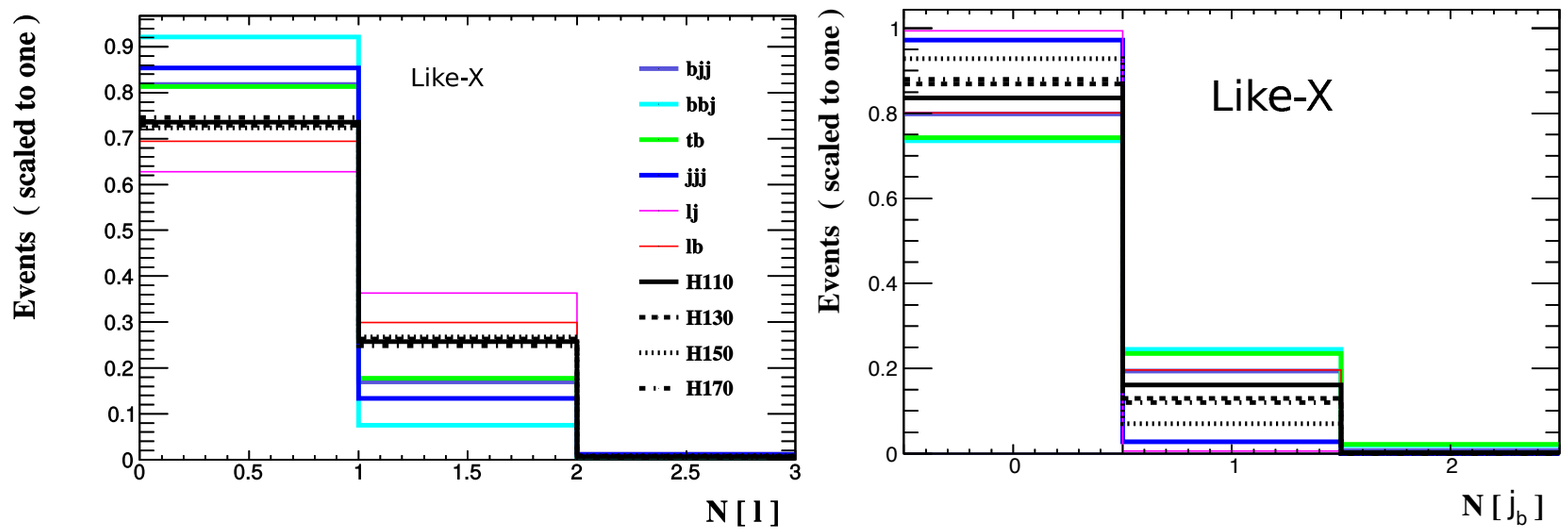

FIG. 9. Distributions for the process $e^- q \to \nu_e H^- b$ followed by $H^- \to \tau \bar{\nu}_\tau$: in the left(right) panel we present the number of leptons(b-jets) per event. The like-X case is illustrated. The normalisation is to unity.

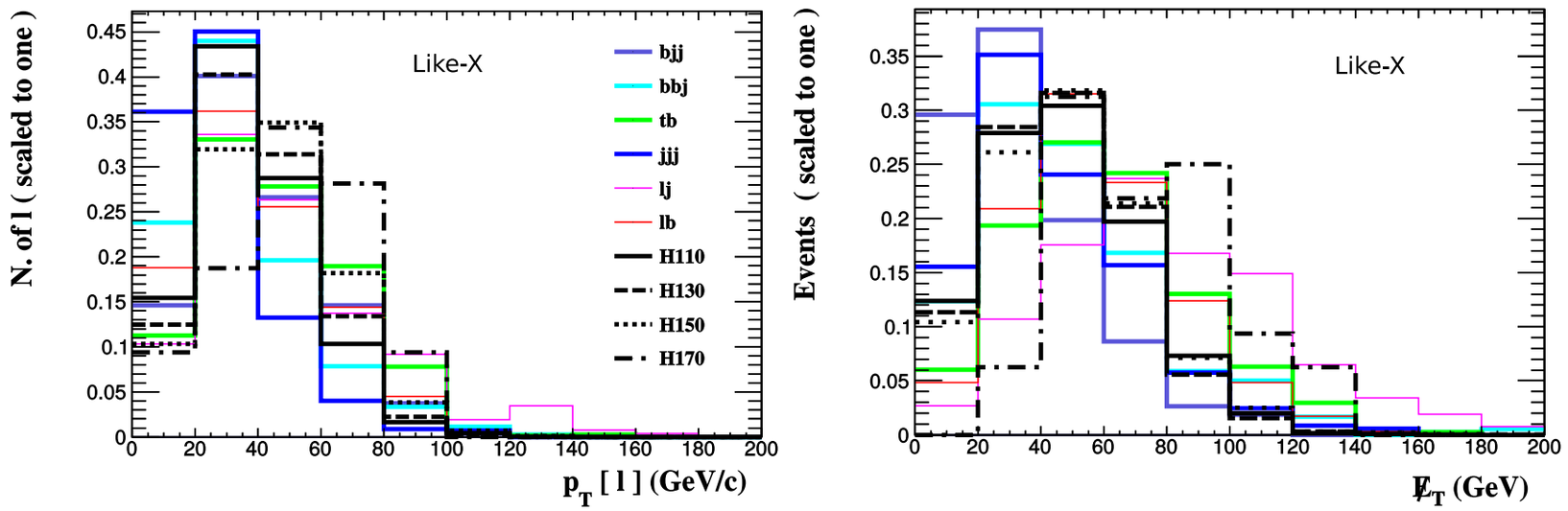

FIG. 10. Distributions for the process $e^- q \to \nu_e H^- b$ followed by $H^- \to \tau \bar{\nu}_\tau$: in the left panel we present the transverse momentum of the lepton while in the right panel we present the total missing transverse energy. The like-X case is illustrated. The normalisation is to unity.

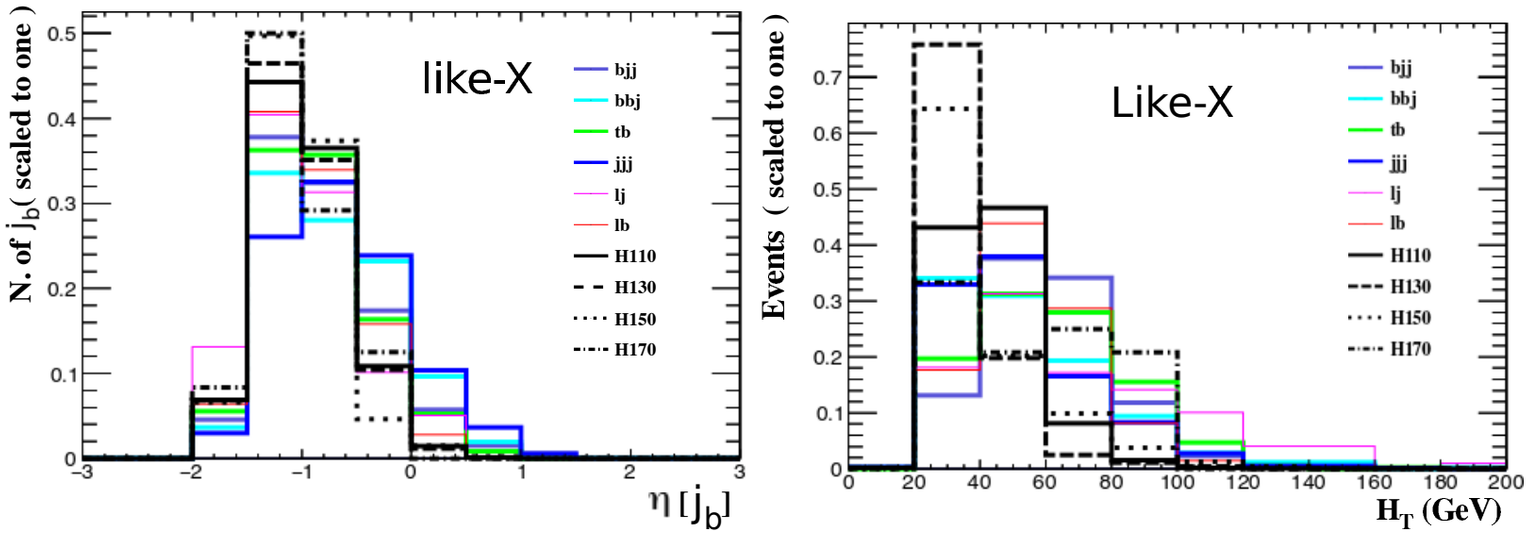

FIG. 11. Distributions for the process $e^- q \to \nu_e H^- b$ followed by $H^- \to \tau \bar{\nu}_\tau$: in the left panel we present the pseudorapidity of the b jet while in the right panel we present the total hadronic transverse energy. The like-X case is illustrated. The normalisation is to unity.

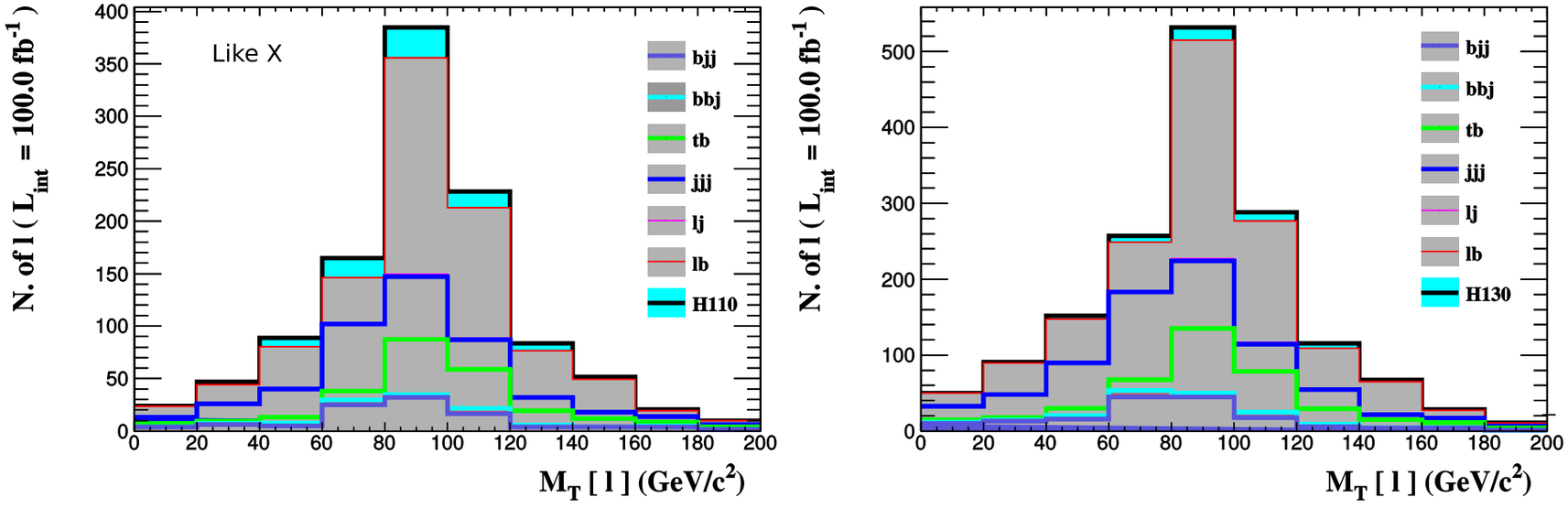

FIG. 12. Distributions for the process $e^- q \to \nu_e H^- b$ followed by $H^- \to \tau \bar{\nu}_\tau$ in the transverse mass of the final state for $m_{H^\pm} = 110$ GeV (left) and $m_{H^\pm} = 130$ GeV (right). The like-X case is illustrated. The normalisation is to the total event rate for $L = 100$ fb^{-1}.

Signal	Scenario	Events (raw)	Cut I	Cut II	Cut III	Cut IV	$(\mathcal{S}/\sqrt{\mathcal{B}})_{100\ \mathrm{fb}^{-1}(1000\ \mathrm{fb}^{-1})[3000\ \mathrm{fb}^{-1}]}$
$\nu_e H^- q$	X-110	6480	178	124	94	67	2.41 (7.61) [13.19]
	X-130	3390	75	54	52	35	1.13 (3.58) [6.2]
	X-150	880	6	3	2	2	0.09 (0.29) [0.5]
	X-170	20	0.4	0.3	0.2	0.09	0.01 (0.02) [0.04]
$\nu_e bbj$		20170	85	56	23	13	
$\nu_e bjj$		117559	623	340	122	84	
$\nu_e tb$		48845	460	374	149	105	$\mathcal{B} = 763$
$\nu_e jjj$		867000	981	596	267	162	$\sqrt{\mathcal{B}} = 27.62$
$\nu_e l\nu_l j$		23700	29	26	8	5	
$\nu_e l\nu_l b$		40400	1500	1203	569	392	

TABLE IV. Significances obtained after the sequential cuts described in the text for the signal process $e^- q \to \nu_e H^- b$ followed by $H^- \to \tau\bar{\nu}_\tau$ for four BPs in the 2HDM-III like-X. The simulation is done at detector level. In the column Scenario, the label X-110(130)[150]{170} means $m_{H^\pm} = 110(130)[150]\{170\}$ GeV in the 2HDM-III like -X.

Probing the $hc\bar{c}$ coupling at a Future Circular Collider in the electron-hadron mode

Point	$X(Z)$	Y	BR($\phi^0 \to ab$)	$\sigma(e^- p \to e^- \phi^0 q)$	Events (1 ab^{-1})
Ia	0.5(0.5) $\mu = 0.88$ $\kappa_c = 1.5$	6.5	BR($h \to b\bar{b}$) = 0.513 BR($h \to c\bar{c}$) = 0.484 BR($h \to sb$) = 1.99×10^{-3} BR($h \to s\bar{s}$) = 8.18×10^{-9}	0.875 pb	2×10^5 2×10^4 52 0
IIa	1(1) $\mu = 1.16$ $\kappa_c = 2$	4	BR($h \to b\bar{b}$) = 0.67 BR($h \to c\bar{c}$) = 0.23 BR($h \to sb$) = 0.093 BR($h \to s\bar{s}$) = 2.87×10^{-3}	0.958 pb	2×10^5 2×10^4 1×10^3 7
Y-min	5(-1/5) $\mu = 0.86$ $\kappa_c = 1.7$	5	BR($h \to b\bar{b}$) = 0.498 BR($h \to c\bar{c}$) = 0.289 BR($h \to sb$) = 0.21 BR($h \to s\bar{s}$) = 1.96×10^{-3}	1.08 pb	2×10^5 2×10^4 7×10^3 5

TABLE III. Relevant cross sections, BRs and event rates (for the machine configuration given in the previous figure caption) for our scenarios Ia, IIa and Y, each mapped in terms of X, Y and Z values. We have included the allowed values for μ and κ_c for each BPs. Here, we have included the following tagging efficiencies in the last column: $\epsilon_b = 0.6$, $\epsilon_c = 0.24$ and $\epsilon_s = 0.05$ [78].

J. Hernandez-Sanchez, C.G. Honorato, Stefano Moretti
Arxiv: 2108.05448, submitted to EJPC.

Background	Cross section [pb]	Number of events
$\nu_e jjj$	172	1.75×10^8
$\nu_e bjj$	16.1	1.61×10^7
$\nu_e bbj$	1.8	1.8×10^6
$\sum \nu 3j$	189.9	10^8
$\nu_e llj$	3.09	3.09×10^6
$\nu_e tb$	12.47	1.24×10^7
$ejjj$	948	9.48×10^8
$ebjj$	17.8	1.78×10^7
$ebbj$	75.4	75.4×10^7
$\sum ejjj$	1040	10^9
ett	0.35	3.5×10^5

TABLE V. Background cross sections and event rates at parton level after the following cuts: $p_T(q) > 10$ GeV, $\Delta R(q,q) > 0.3$ and $|\eta(q)| < 7$ (assuming the usual FCC-eh parameters).

the effective di-jet final state defined above as $N_j + N_{b\to j} + N_{c\to j}$

Signal	Raw events	Sim Events	Set **A)**	Set **B)**	Set **C)**	Set **D)**	Set **E)**	Significance
Ia	875000	890530	633866	190986	91117	77079	36054	36.3
			36075	10869	5186	4387	2052	8.31
IIa	958000	970336	609152	178088	87714	72312	30898	31.19
			32350	9457	4658	3840	1641	6.67
Y	1070000	1085244	736138	208665	101427	83083	35824	36.08
			41941	11884	5776	4732	2040	8.27
$\Sigma\nu 3j$	1.89×10^8	19956113	176368197	40956844	9327890	4960087	820718	
			10334771	2399977	546593	290650	48092	
νtb	1.24×10^7	1254485	7880059	1505048	759201	548492	123961	
			501285	95743	48296	34892	7886	$\Sigma\, B =$
$\Sigma e3j$	10^9	104495242	73393857	3093729	29137	24770	2750	950207
			52792574	2225334	20958	17817	1978	58865
ett	350000	353583	26046	380	109	77	21	
			14764	215	62	44	12	
$\Sigma\nu llj$	3090000	1434318	411923	117562	29915	19052	2757	
			134029	38253	9733	6199	897	

TABLE VI. Cutflow for all signals and backgrounds. Here, in each cell, the top line represents the number of light di-jet events while the bottom one refers to those enriched by $c\bar{c}$ states, as described in the text.

$N_{b\to j}$. (In fact, the latter also includes a $\propto (1-\epsilon_b)$

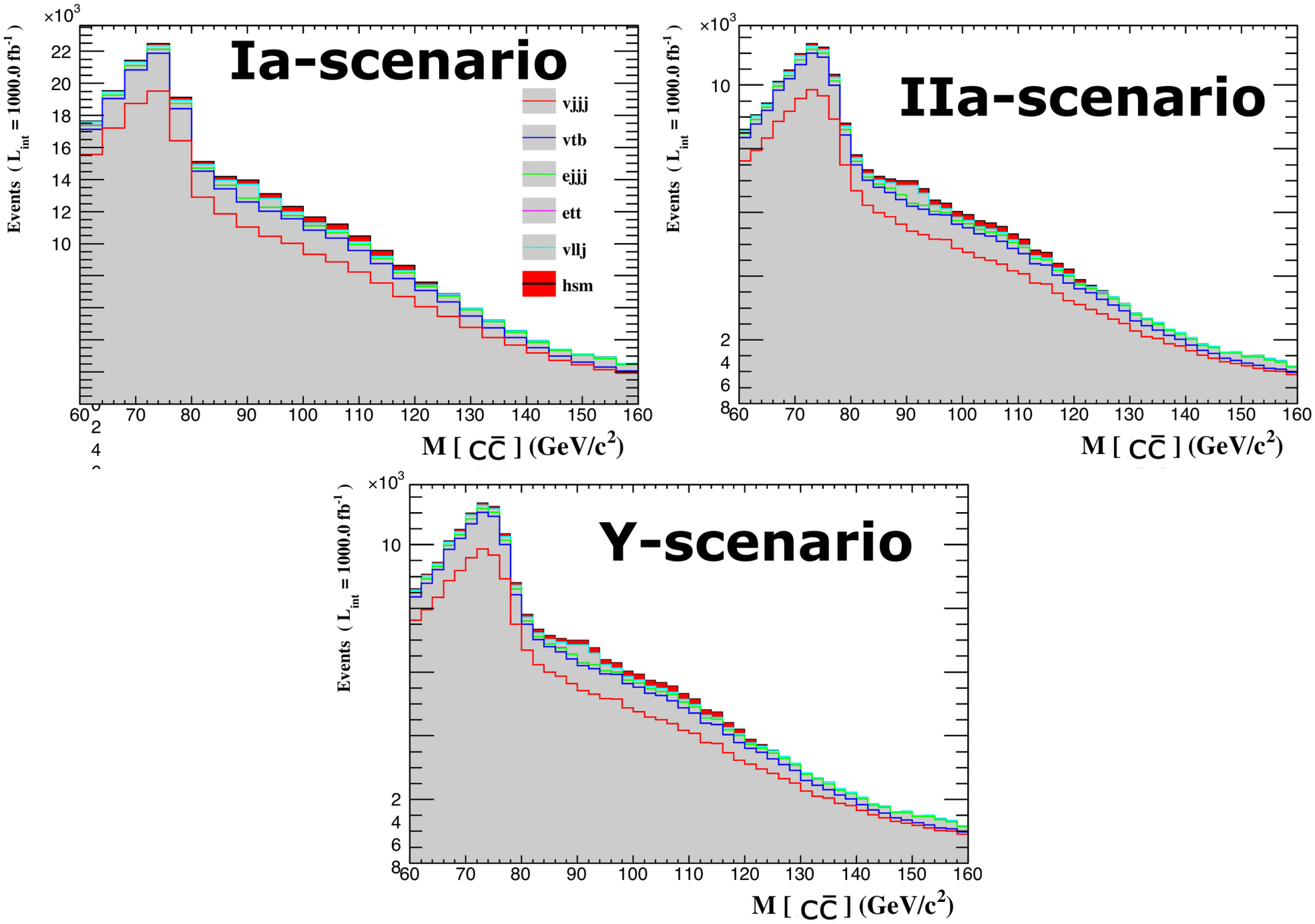

FIG. 5. Di-jet invariant mass distribution. These histograms are made for the Ia (top-left), IIa (top-right) and Y (bottom) incarnations of the 2HDM-III signal (red histogram) as well as the five categories of background discussed in the text (here stacked beneath the signal). Here, we present the rates for the case of $c\bar{c}$-tagged sample.

Summary

We study the 2HDM-III as effective Lagrangian that induce flavor violating signatures and interesting signals like h,H —> sb.

We study the signal h,H —> sb in the future ep collider LHeC: e p —> q nu h. We have a significance up to 5 for h SM-like and for H with mass 130-150 GeV: a significance around to 4 for both colliders LHeC and FCC-eh.

Our study is consistent with flavor physics, Higgs physics and EWPO.

Following the some strategies for the neutral Higgs boson, we study the production of H+ in the channel cb for the future ep collider LHeC and extrapolate our results for FCC-eh.

We show some results for H- —>cb. We have sufficient event rates in order to get a significance 4.18 at 100 fb^-1 (6.89 at1000 fb^-1) for LHeC. For FCC-eh, the significance could reach 11.2 at 1000 fb^-1

We study the signal h —> cc in the future ep collider FCCeh.